

# Superconductivity and topological properties in the kagome metals $\text{CsM}_3\text{Te}_5$ ( $M=\text{Ti, Zr, Hf}$ ): A first-principles investigation

Jian-Guo Si<sup>1,2,\*</sup>, Lan-Ting Shi<sup>1,2,\*</sup>, Peng-Fei Liu<sup>1,2</sup>, Ping Zhang<sup>3,4</sup> and Bao-Tian Wang<sup>1,2,3,5,†</sup>

<sup>1</sup>*Institute of High Energy Physics, Chinese Academy of Sciences, Beijing 100049, China*

<sup>2</sup>*Spallation Neutron Source Science Center, Dongguan 523803, China*

<sup>3</sup>*School of Physics and Physical Engineering, Qufu Normal University, Qufu 273165, China*

<sup>4</sup>*Institute of Applied Physics and Computational Mathematics, Beijing 100088, China*

<sup>5</sup>*Collaborative Innovation Center of Extreme Optics, Shanxi University, Taiyuan, Shanxi 030006, China*



(Received 10 May 2022; revised 25 October 2022; accepted 15 December 2022; published 28 December 2022)

Inspired by the discovery and fascinating properties of kagome metals  $\text{AV}_3\text{Sb}_5$  ( $A = \text{K, Rb, Cs}$ ), we investigate the superconductivity and topological properties of the  $\text{AV}_3\text{Sb}_5$ -prototype kagome materials  $\text{CsM}_3\text{Te}_5$  ( $M = \text{Ti, Zr, Hf}$ ) using first-principles calculations. The calculated results of formation energy and phonon dispersion indicate that this family of kagome materials are stable and may be synthesized in experiments. By analytically solving the Allen-Dynes-modified McMillan formula, the superconducting critical temperatures for  $\text{CsTi}_3\text{Te}_5$ ,  $\text{CsZr}_3\text{Te}_5$ , and  $\text{CsHf}_3\text{Te}_5$  are predicted as 8.02, 5.47, and 3.51 K, respectively. The electron-phonon couplings are dominated by the coupling between the in-plane atomic vibrational modes and the in-plane electronic orbitals. In addition, the  $\text{CsZr}_3\text{Te}_5$  and  $\text{CsHf}_3\text{Te}_5$  can be categorized as  $\mathbb{Z}_2$  topological metals according to the calculations of topological invariant and surface states. Such coexistence of superconductivity and nontrivial topological properties in  $\text{CsZr}_3\text{Te}_5$  and  $\text{CsHf}_3\text{Te}_5$  are beneficial to study the interaction between superconductivity and nontrivial band character.

DOI: [10.1103/PhysRevB.106.214527](https://doi.org/10.1103/PhysRevB.106.214527)

## I. INTRODUCTION

The kagome lattice with inherent geometrical frustration offers an ideal platform to study intriguing phenomena, such as magnetic topological states [1–4], spin liquid states [5,6], anomalous Hall effect [7–9], superconductivity [10–13], chiral physics [14–16], etc. In momentum space, the typical tight-binding calculations of the kagome lattice manifest that its band structure coexists with a flat band over the Brillouin zone (BZ), a Dirac-type band crossing at  $K$  point and a van Hove point at the  $M$  point [2,16,17], which have been partially identified by the angle resolved photoemission spectroscopy (ARPES) measurements [17–20] and the scanning tunneling microscopy experiments [21,22]. Therefore, theoretically predicting and experimentally synthesizing new kagome materials, and further exploring their unconventional physical properties are important in both condensed-matter physics and material physics.

Recently, a new family of V-based kagome metals  $\text{AV}_3\text{Sb}_5$  ( $A = \text{K, Rb, Cs}$ ) have been synthesized with a quasi-two-dimensional characteristics [23]. Decreasing the temperature,  $\text{AV}_3\text{Sb}_5$  family materials undergo charge density wave (CDW) transitions in range of 80 to 102 K [24–30]. The CDW order was, subsequently, turned out to exhibit a kind of unconventional chiral feature [15,26,31]. By further decreasing the temperature, the systems will enter in a superconduct-

ing ground state. The superconducting transition temperatures  $T_c$  were reported to be 0.93, 0.92, and 2.5 K for  $\text{KV}_3\text{Sb}_5$ ,  $\text{RbV}_3\text{Sb}_5$ ,  $\text{CsV}_3\text{Sb}_5$  [11,24–26,30], respectively. Under low pressure, monotonic suppression of the CDW order was detected, whereas the superconductivity exhibits a reemergence character in  $\text{CsV}_3\text{Sb}_5$  [32]. Under higher pressure, the superconducting transition temperature shows double-dome-like pressure-dependent behaviors [13,30,33,34]. The effects of strain [35], doping [36], and dimensional reducing [37,38] on the CDW and superconductivity have also been investigated. Besides, theoretical calculations have predicted that the  $\text{AV}_3\text{Sb}_5$  family kagome materials exhibit nontrivial band crossing around the Fermi level [11,23,25], which was subsequently confirmed by the ARPES and Shubnikov–de Haas oscillation experiments [11,24,27,39].

If the superconductivity materials could coexist with a nontrivial band structure, they can be regarded as promising candidates for realizing topological superconductors. There will be some novel quantum phases in topological superconductors, such as the Majorana zero mode [40–42], which can be used in quantum information processing [43]. For the  $\text{CsV}_3\text{Sb}_5$ , the Majorana bound states (MBSs) have been successfully detected [29], providing the first glimpse into Majorana modes in  $\text{AV}_3\text{Sb}_5$  family materials. Through investigating the pairing symmetry theoretically, Ding *et al.* found that the MBSs in the vortex core should only appear with the chiral  $p$ -wave pairing [44]. Such rich quantum phenomena in the  $\text{AV}_3\text{Sb}_5$  family spark intense research interest on kagome materials.

To explore more kagome compounds with the coexistence of superconductivity and nontrivial band structure, we predict

\*These authors contributed equally to this work.

†Author to whom correspondence should be addressed; wangbt@ihep.ac.cn

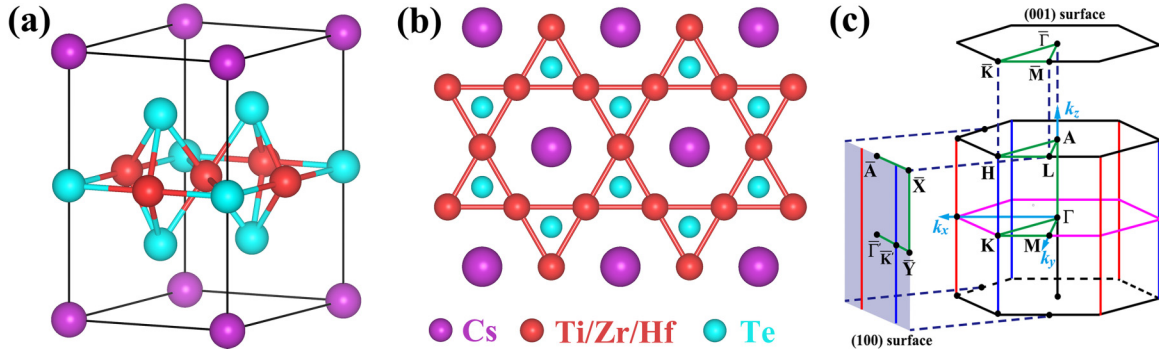


FIG. 1. (a) Side and (b) top views of the crystal structure of  $\text{CsM}_3\text{Te}_5$ . The purple, red, and turquoise balls indicate the Cs, transition-metal Ti/Zr/Hf, and Te atoms, respectively. (c) Bulk BZ and the high-symmetry path used in band-structure calculations. The project (001) and (100) surfaces are also plotted.

some  $\text{AV}_3\text{Sb}_5$ -type materials and then check their stability and investigate their electronic structures, superconductivity, and topological properties using first-principles calculations. Among all our tested systems, the  $\text{CsM}_3\text{Te}_5$  ( $M=\text{Ti, Zr, Hf}$ ) exhibit good stability and properties. The calculated results of formation energy are significantly larger than that of  $\text{CsV}_3\text{Sb}_5$ , indicating that these compounds are stable and can be easily synthesized in experiments. The phonon dispersions results indicate that there is no potential CDW transition in these systems. The superconductivity is estimated based on the Allen-Dynes-modified McMillan formula [45,46] with superconducting transition temperatures of 8.02, 5.47, and 3.51 K for  $\text{CsTi}_3\text{Te}_5$ ,  $\text{CsZr}_3\text{Te}_5$ , and  $\text{CsHf}_3\text{Te}_5$ , respectively, which are higher than those of the  $\text{AV}_3\text{Sb}_5$  family materials. Similar to  $\text{AV}_3\text{Sb}_5$ , the  $\text{CsZr}_3\text{Te}_5$  and  $\text{CsHf}_3\text{Te}_5$  are also predicted as  $\mathbb{Z}_2$ -topological metals by calculating the topological invariant and surface states. The coexistence of superconductivity and nontrivial topological properties in  $\text{CsZr}_3\text{Te}_5$  and  $\text{CsHf}_3\text{Te}_5$  supply guidance for further theoretical and experimental works to seek novel topological nature in superconducting materials, especially in materials with the  $\text{AV}_3\text{Sb}_5$ -prototype structure.

## II. COMPUTATIONAL DETAILS

Our first-principles calculations were performed in the density functional theory (DFT) level via the QUANTUM ESPRESSO package [47]. The ultrasoft pseudopotentials were used to treat the interaction between the electrons and the ionic cores [48] where the exchange-correlation interaction was described by the generalized gradient approximation and parametrized by the Perdew-Burke-Ernzerhof functional [49]. The zero damping DFT-D3 functional was employed to consider the van der Waals (vdW) correction [50], which was proved to be accurate in the isostructural  $\text{AV}_3\text{Sb}_5$  family materials [51–53]. The cutoff energy of wave functions and charge density were set as 60 and 600 Ry, respectively. To calculate the charge density, the Gaussian smearing method was used with a smearing parameter of  $\sigma = 0.01$  Ry. The convergence criterion for self-consistent calculations was set as  $10^{-6}$  Ry. The BZ was sampled on a  $16 \times 16 \times 12$  mesh of  $k$  points for structural optimization, and all structures were fully relaxed until the force acting on each atom is less than  $10^{-5}$  Ry/Å.

Phonon dispersion curves were calculated based on the density functional perturbation theory [54] where a denser  $20 \times 20 \times 12$   $k$ -point grid and a  $5 \times 5 \times 3$   $q$ -point grid were employed for the electron-phonon coupling (EPC) calculations. The phonon-related calculations were carried out without including the spin-orbit coupling (SOC) effect due to it is less important in describing the vibrational and superconductivity properties [55,56]. The iterative Green's function was used to calculate the surface states as implemented in the WANNIERTOOLS package [57,58] where the tight-binding method was employed with the maximally localized Wannier function [59,60].

## III. RESULTS AND DISCUSSION

The  $\text{CsM}_3\text{Te}_5$  family materials are constructed by partly atoms substituting of prototype structure  $\text{AV}_3\text{Sb}_5$  where the V atoms are replaced by the transition metals  $M$  ( $M=\text{Ti, Zr, Hf}$ ) and the Sb atoms are replaced by Te atoms. Such atom substitution is a normal method used in synthesizing new material. For example, the  $\text{CsAg}_5\text{Te}_3$  was reported as a thermoelectric material with ultralow thermal conductivity [61]. Through elemental substituting, the  $\text{CsCu}_5\text{S}_3$  [62] and  $\text{CsCu}_5\text{Se}_3$  [63] were successfully prepared with the same structure. As shown in Fig. 1, the  $\text{CsM}_3\text{Te}_5$  systems crystallize in a hexagonal space group of  $P6/mmm$  (No. 191). One can see that the  $M_3\text{Te}_5$  slabs stack along the  $c$  axis through vdW interactions, whereas the Cs atoms insert into the adjacent  $M_3\text{Te}_5$  slabs. The transition-metals Ti/Zr/Hf atoms form the kagome structure. The fully optimized parameters are listed in Table I. It can be seen that the lattice parameter along the  $c$  direction increases with the increase in the atomic number, and the  $\text{CsZr}_3\text{Te}_5$  has the largest in-plane lattice parameters

TABLE I. Crystal parameters (in angstroms) and the formation energy (in eV) of  $\text{CsM}_3\text{Te}_5$  and  $\text{CsV}_3\text{Sb}_5$ .

	$a$	$c$	$E_{\text{formation}}$
$\text{CsTi}_3\text{Te}_5$	6.057	8.456	-1.299
$\text{CsZr}_3\text{Te}_5$	6.362	8.572	-1.433
$\text{CsHf}_3\text{Te}_5$	6.282	8.651	-1.340
$\text{CsV}_3\text{Sb}_5$	5.454	9.330	-0.410

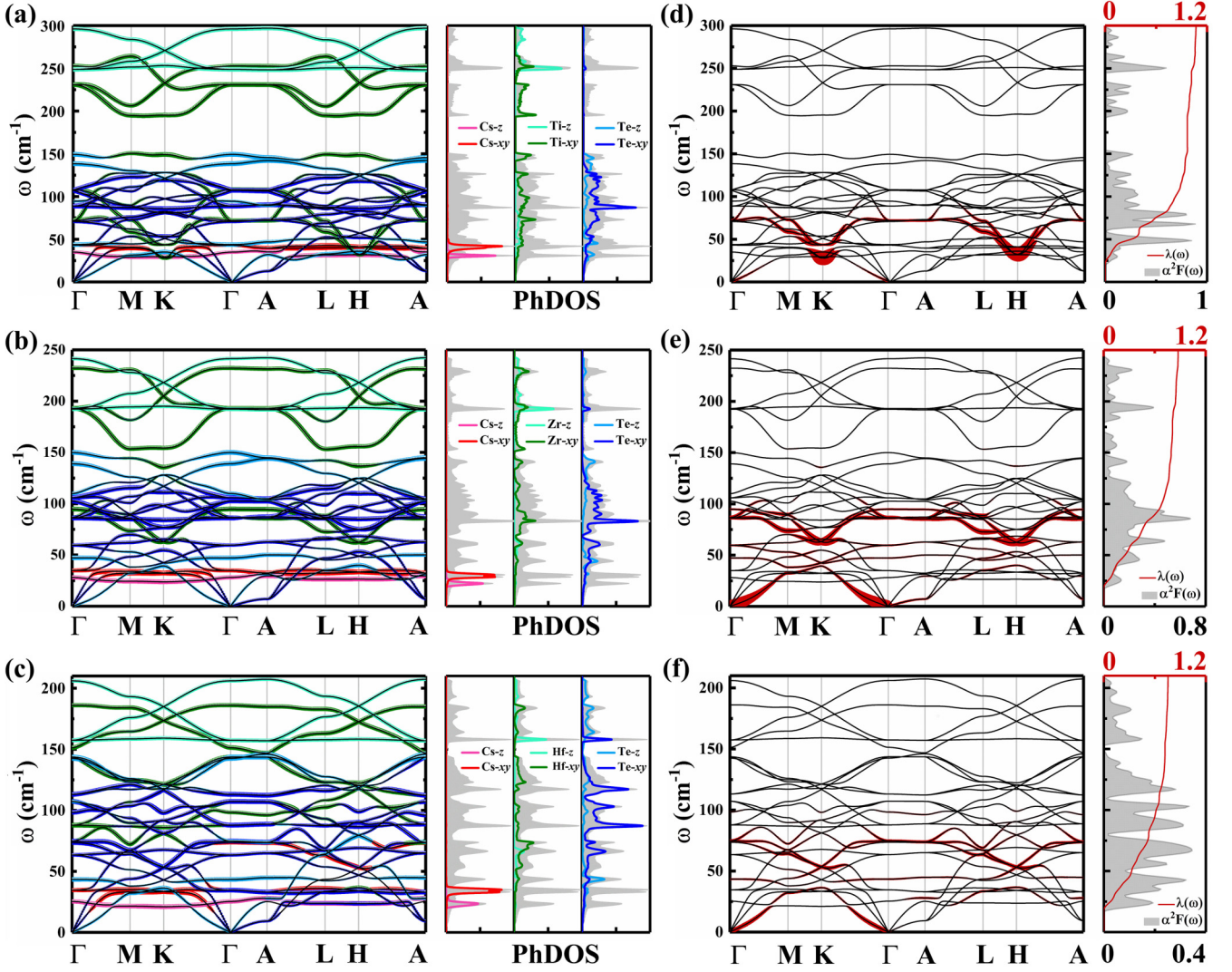


FIG. 2. Phonon dispersions weighted by different atomic vibrational modes of (a)  $\text{CsTi}_3\text{Te}_5$ , (b)  $\text{CsZr}_3\text{Te}_5$  and (c)  $\text{CsHf}_3\text{Te}_5$ . The right panels of (a)–(c) are the total (gray-shaded zone) and vibrational mode-resolved (colored lines) phonon density of states (PhDOS). Phonon dispersions weighted by the magnitude of the EPC, the Eliashberg spectral function  $\alpha^2F(\omega)$ , and the integrated strength of EPC  $\lambda(\omega)$  for (d)  $\text{CsTi}_3\text{Te}_5$ , (e)  $\text{CsZr}_3\text{Te}_5$ , and (f)  $\text{CsHf}_3\text{Te}_5$  are also presented.

of  $a$ . Our calculated parameters are slightly smaller than those reported in one recent DFT work [64] where the vdW correlations were ignored.

To evaluate the thermal stability of  $\text{CsM}_3\text{Te}_5$ , we calculate the formation energy by

$$E_{\text{formation}} = \frac{E_{\text{CsM}_3\text{Te}_5} - E_{\text{Cs}} - 3E_{\text{M}} - 5E_{\text{Te}}}{9}. \quad (1)$$

Here,  $E_{\text{CsM}_3\text{Te}_5}$  is the total energy of  $\text{CsM}_3\text{Te}_5$ , and  $E_{\text{Cs}}$ ,  $E_{\text{M}}$ , and  $E_{\text{Te}}$  are the energies of the stable elemental Cs, transition metals, and Te, respectively. The calculated results are listed in Table I. One can see that all of them have negative formation energies, indicating their thermal stability. For comparison, we also calculate the formation energy of the kagome metal  $\text{CsV}_3\text{Sb}_5$ , which has been synthesized experimentally. As clearly indicated in Table I, the formation energies of the predicted  $\text{CsM}_3\text{Te}_5$  are evidently lower than that of  $\text{CsV}_3\text{Sb}_5$ . To further prove the stability, we perform a structure search of Cs- $M$ -Te ( $M=\text{Ti}$ , Zr, Hf) systems in the Supplemental

Material [65] (also see references [66–73] therein), where only one Cs is considered, the ratio of the transition-metal  $M$  atoms are in range of 2 to 3 and the ratios of Te atoms are in the range of 2–5. The calculated results of convex hull diagrams are drawn in Fig. S1 of the Supplemental Material [65]. All of the results indicate that the most stable structure with a stoichiometric ratio of “135” is the structure in the space group of  $P6/mmm$ . Thus, we can expect that the kagome materials  $\text{CsM}_3\text{Te}_5$  should be synthesized under suitable external conditions.

Figure 2 shows the phonon dispersion curves of  $\text{CsM}_3\text{Te}_5$ . We can see that there is no imaginary phonon mode for these three compounds, indicating that they are dynamically stable. In the low-frequency region, the vibration modes of Cs atoms form two flat phonon bands, accompanying with two sharp peaks in the PhDOS. The midfrequency region is mainly dominated by the vibration modes of Te atoms with some contributions from the transition-metal atoms. There is an optic phonon gap of  $44.6 \text{ cm}^{-1}$  for  $\text{CsTi}_3\text{Te}_5$ . Such a gap

decreases with the increase in the weight of the transition metals and disappears in  $\text{CsHf}_3\text{Te}_5$ . For the high-frequency region, the phonon originates mainly from the transition-metal atoms. The out-of-plane vibration modes of the transition metals form a very flat band. Such a phonon flat band character was also found in the isostructural  $\text{CsV}_3\text{Sb}_5$  [52], which may induce more interesting phenomena. As mentioned above, the kagome metal  $\text{AV}_3\text{Sb}_5$  family materials show the coexistence of CDW, superconductivity, and nontrivial topological properties. It has been proved that the calculation of phonon dispersion is an effective method to evaluate the CDW instability [74,75]. For our studied  $\text{CsM}_3\text{Te}_5$ , there is no imaginary in their phonon dispersions, indicating that these materials will not undergo the CDW transition [76]. Therefore, we will focus on the superconductivity and topological properties in them.

The superconductivity of  $\text{CsM}_3\text{Te}_5$  are estimated by the EPC calculations. The superconducting transition temperature  $T_c$  is calculated based on the Allen-Dynes-modified McMillan formula [45,46],

$$T_c = \frac{\omega_{\log}}{1.2} \exp\left(-\frac{1.04(1+\lambda)}{\lambda - \mu^* - 0.62\lambda\mu^*}\right), \quad (2)$$

where the  $\mu^*$  is the effective Coulomb pseudopotential and can be set as a typical value of 0.1 [52,77]. The integrated EPC constant can be evaluated by

$$\lambda(\omega) = 2 \int \frac{\alpha^2 F(\omega)}{\omega} d\omega. \quad (3)$$

Here, the Eliashberg spectral function  $\alpha^2 F(\omega)$  is calculated according to the following formula:

$$\alpha^2 F(\omega) = \frac{1}{2\pi N(E_F)} \sum_{qv} \delta(\omega - \omega_{qv}) \frac{\gamma_{qv}}{\hbar\omega_{qv}}, \quad (4)$$

where  $\omega_{qv}$  are phonon frequencies,  $\gamma_{qv}$  is the phonon linewidth as described by

$$\gamma_{qv} = 2\pi\omega_{qv} \sum_{ij} \int \frac{d^3k}{\Omega_{BZ}} |g_{qv}(k, i, j)|^2 \times \delta(\varepsilon_{q,i} - \varepsilon_F) \delta(\varepsilon_{k+q,j} - \varepsilon_F). \quad (5)$$

Here,  $g_{qv}(k, i, j)$  is the matrix of the EPC, and  $\varepsilon_{q,i}$  is the electronic energy. The calculated Eliashberg spectral and the integrated strength of the EPC are plotted in Figs. 2(d)–2(f). As shown, the integrated strength of the EPC below 100  $\text{cm}^{-1}$  reaches 78.1%, 78.3%, and 81.8% of the total EPCs for  $\text{CsTi}_3\text{Te}_5$ ,  $\text{CsZr}_3\text{Te}_5$ , and  $\text{CsHf}_3\text{Te}_5$ , respectively. Although the distributions of  $\alpha^2 F(\omega)$  are non-negligible at the high-frequency region (above 100  $\text{cm}^{-1}$ ), their contribution to the EPC is limited. Such phenomena can be easily understood by Eq. (3). The calculated total  $\lambda$ 's are 1.07, 0.88, and 0.75 for  $\text{CsTi}_3\text{Te}_5$ ,  $\text{CsZr}_3\text{Te}_5$ , and  $\text{CsHf}_3\text{Te}_5$ , respectively. Thus,  $\text{CsTi}_3\text{Te}_5$  can be regarded as a medium-coupling conventional superconductor, whereas  $\text{CsZr}_3\text{Te}_5$  and  $\text{CsHf}_3\text{Te}_5$  are weak conventional superconductors.

The  $\omega_{\log}$  in Eq. (2) is the logarithmically averaged characteristic phonon frequency, which is defined as

$$\omega_{\log} = \exp\left(\frac{2}{\lambda} \int \frac{d\omega}{\omega} \alpha^2 F(\omega) \log \omega\right). \quad (6)$$

TABLE II. Calculated electronic DOS at the Fermi level  $N(E_F)$  (in states/eV), strength of EPC ( $\lambda$ ),  $\omega_{\log}$ , and superconducting transition temperature ( $T_c$  in K) for  $\text{CsM}_3\text{Te}_5$ .

	$N(E_F)$	$\lambda$	$\omega_{\log}$	$T_c$
$\text{CsTi}_3\text{Te}_5$	2.85	1.07	103.63	8.02
$\text{CsZr}_3\text{Te}_5$	2.34	0.88	97.77	5.47
$\text{CsHf}_3\text{Te}_5$	2.18	0.75	93.04	3.51

Taking  $\lambda$  and  $\omega_{\log}$  into Eq. (2), one can obtain the superconducting transition temperature. The calculated  $T_c$  as well as superconducting parameters of  $\lambda$  and  $\omega_{\log}$  are listed in Table II. For these three compounds,  $\lambda$ ,  $\omega_{\log}$ , and  $T_c$  have the same trend: decreasing with the increase in the atomic number.  $\text{CsTi}_3\text{Te}_5$  has the largest  $\lambda$  as well as the largest superconducting transition temperature  $T_c$  of 8.02 K, which is three times larger than those of the  $\text{AV}_3\text{Sb}_5$  family materials [30,32–34]. In one recent DFT work, the  $T_c$  of  $\text{CsZr}_3\text{Te}_5$  was predicted as 1.27 K [78]. Such large differences between their results and ours may need further experiments to verify.

The phonon dispersions weighted by the magnitude of EPC are drawn in Figs. 2(d)–2(f). To obtain the modes' contribution to the superconductivity of these three compounds, we compare the phonon dispersions weighted by vibration modes of different atoms in Figs. 2(a)–2(c) with the distribution and strength of the EPC. For  $\text{CsTi}_3\text{Te}_5$ , the softened modes around the  $K$  and  $H$  points show obvious EPC, which is dominated by the in-plane vibration modes of Ti  $xy$ . When it comes to  $\text{CsZr}_3\text{Te}_5$  and  $\text{CsHf}_3\text{Te}_5$ , the EPC becomes more homogeneous, and the vibration modes of Te atoms have more and more contributions to the EPC, especially the in-plane one. These results are also consistent with the flat phonon bands and peaks of  $\alpha^2 F(\omega)$  for frequency below 100  $\text{cm}^{-1}$ . The delocalization of the EPC with increasing atomic number is similar to the case of kagome metal  $\text{CsV}_3\text{Sb}_5$  under pressure [52].

After confirming the superconductivity in our studied systems, we now want to investigate their electronic structures and topological states. The band structures without considering the SOC effect are shown in Figs. 3(a)–3(c). As expected, the Dirac-like band crossing points for these three kagome compounds locate at the  $K$  and  $H$  points. For  $\text{CsTi}_3\text{Te}_5$ , the Dirac point at the  $H$  point is just on the Fermi level, whereas the one at the  $K$  point is  $-160$  meV below the Fermi level. Besides, the lower half band of the Dirac point does not cross the Fermi level. As shown by the green lines in Figs. 3(b) and 3(c), the lower bands of the Dirac point for  $\text{CsZr}_3\text{Te}_5$  and  $\text{CsHf}_3\text{Te}_5$  do cross the Fermi level. This means that the dispersions of the Fermi-level crossed bands are enhanced with the increase in the atomic number. The movement of Dirac-like band crossing points may be attributed to the change in the Fermi energy. At  $M$  and  $L$  points, the van Hove singularities are detected. Comparing with  $\text{CsV}_3\text{Sb}_5$ , the van Hove singularities in  $\text{CsM}_3\text{Te}_5$  are farther from the Fermi level. This kind of Dirac-like band crossing points and van Hove singularities are consistent with the traditional kagome materials [2,16,17].

The calculated DOS are shown in Figs. 3(d)–3(f). One can see that the  $d$  electrons of the transition metals and the  $p$

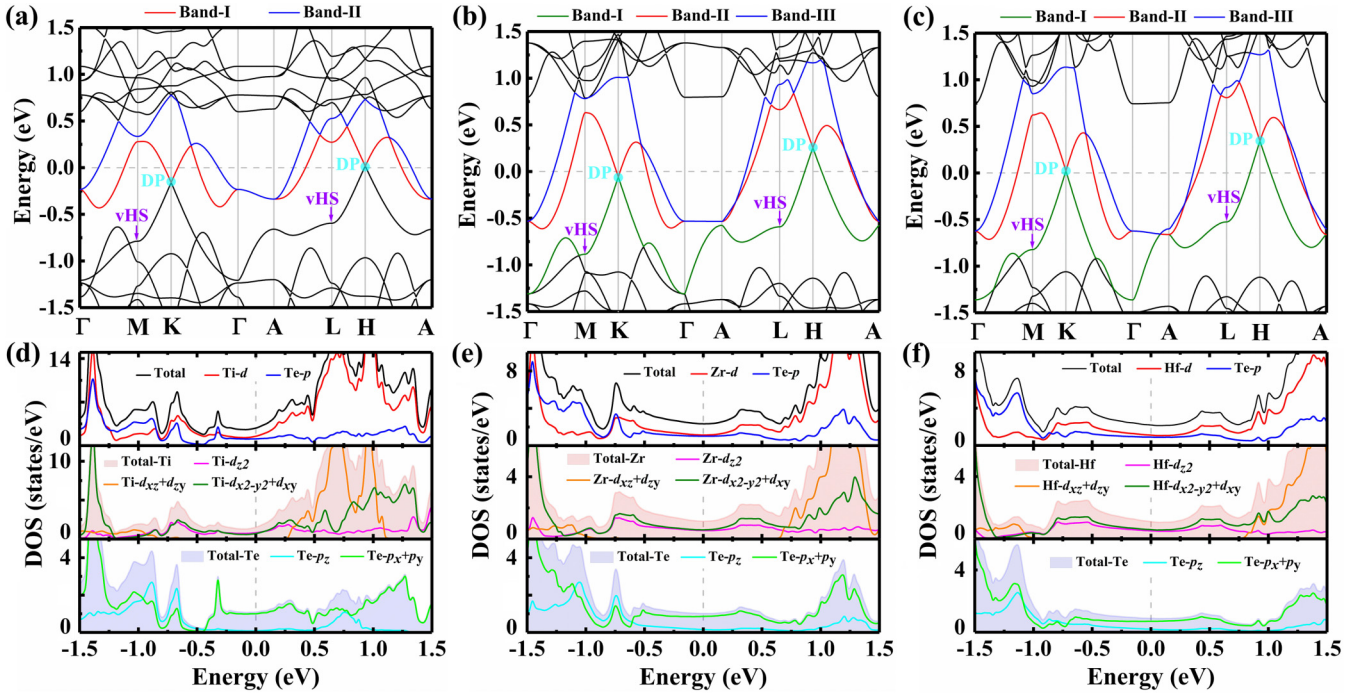


FIG. 3. Band structures without the SOC effect of (a)  $\text{CsTi}_3\text{Te}_5$ , (b)  $\text{CsZr}_3\text{Te}_5$ , and (c)  $\text{CsHf}_3\text{Te}_5$ . The colored lines indicate the bands crossing the Fermi level. The Dirac points and the van Hove singularities are illustrated by the light-blue circles and the purple arrows, respectively. (d) The top panel is the total DOS and the atom-resolved DOSs. The middle and bottom panels are the orbital-resolved DOSs of Ti and Te, respectively. (e) and (f) The same as (d) but for  $\text{CsZr}_3\text{Te}_5$  and  $\text{CsHf}_3\text{Te}_5$ , respectively.

electrons of Te atoms contribute almost equally to the total DOS at the Fermi energy. The contribution of Cs atoms is negligible. The calculated DOS at the Fermi energy  $N(E_F)$  are listed in Table II. We can see that the  $N(E_F)$  exhibits the same trend as those of  $\lambda$ ,  $\omega_{10g}$ , and  $T_c$ , decreasing with the increasing atomic number. Based on the original form of the BCS theory [79,80], we can conclude the change in  $N(E_F)$  is an important factor to the modulation of  $T_c$ . A similar relation between  $N(E_F)$  and  $T_c$  has also been found in our previous study of Zr [81] and two-dimensional metal hexaborides [82]. To obtain accurate orbital distribution, the orbital-resolved DOS are calculated and are presented in Figs. 3(d)–3(f). Comparing to the out-of-plane orbitals  $d_{xz}/d_{yz}$ , the in-plane orbitals  $d_{xy}/d_{x^2-y^2}$  and the  $d_{z^2}$  orbitals of the transition-metal atoms contribute dominantly around the Fermi level. For Te atoms, the in-plane orbitals  $p_x/p_y$  also have larger contributions than the  $p_z$  orbital. Recalling the modes' contribution to the superconductivity mentioned above, we can attribute the superconductivity in these three kagome materials to the coupling between in-plane atomic vibration modes and in-plane electronic orbitals.

By analyzing the parity of the wave function at the time-reversal invariant momentum (TRIM) points and the surface states, the kagome material  $\text{CsV}_3\text{Sb}_5$  was reported as the  $\mathbb{Z}_2$ -topological metal [51]. Here, we also investigate the topological properties with including the SOC effect. Figure 4 shows the band structures of  $\text{CsM}_3\text{Te}_5$  with SOC. One can see that the van Hove singularities are robust existing at the  $M$  and  $L$  points for  $\text{CsTi}_3\text{Te}_5$  and  $\text{CsHf}_3\text{Te}_5$ . But for  $\text{CsZr}_3\text{Te}_5$ , the van Hove singularity at the  $M$  point moves to the  $\Gamma$ - $K$  direction. Besides, after including SOC, two continuous band

gaps are formed across the whole BZ at the Fermi level. For  $\text{CsTi}_3\text{Te}_5$ , the Dirac-like band crossing points are gapped about 12 meV. With increasing the mass of transition metals, the gaps at  $K$  and  $H$  points are enhanced to 24 (38) and 80 (146) meV for  $\text{CsZr}_3\text{Te}_5$  ( $\text{CsHf}_3\text{Te}_5$ ), respectively. Similar to the kagome metal  $\text{CsV}_3\text{Sb}_5$  [51], the  $\text{CsM}_3\text{Te}_5$  family materials persist both inversion and time-reversal symmetries. Given the continuous band gaps across the whole BZ, we can calculate the  $\mathbb{Z}_2$  indices of each bands around the Fermi level via analyzing the parity of the wave function at the eight TRIM points [51,83]. The calculated results are listed in Table III. These results indicate that  $\text{CsZr}_3\text{Te}_5$  and  $\text{CsHf}_3\text{Te}_5$  are topological nontrivial, whereas  $\text{CsTi}_3\text{Te}_5$  is topological trivial. For those two nontrivial materials, we further calculate their surface states on the (001) surface (see Fig. 5), which is the easy cleavage surface with the vdW interactions. One can see obviously that surface states of the (001) plane are 0.7 eV below the Fermi level, which is consistent with a recent report for  $\text{CsZr}_3\text{Te}_5$  [78]. Such surface states can be raised closer to the Fermi level by charge doping or high pressure and further detected by the ARPES measurements. We also plot the surface states on the (100) plane as shown in Figs. 5(b) and 5(d). For  $\text{CsZr}_3\text{Te}_5$ , one can see that the surface states along the  $\bar{\Gamma}'$ - $\bar{K}'$  direction are 50 meV below the Fermi level, which start from the gap at the  $K$  point. Along the  $\bar{K}'$ - $\bar{X}$  direction, the surface states are splitted. When it comes to the case of  $\text{CsHf}_3\text{Te}_5$ , the surface along  $\bar{\Gamma}'$ - $\bar{K}'$  are melted into the bulk bands, but it still can be tracked from the  $\bar{\Gamma}'$  point. Comparing to the  $\text{CsZr}_3\text{Te}_5$ , the surface states along the  $\bar{K}'$ - $\bar{X}$  direction are not splitted. These complicated surface states may induce more interesting phenomena in their transport properties.

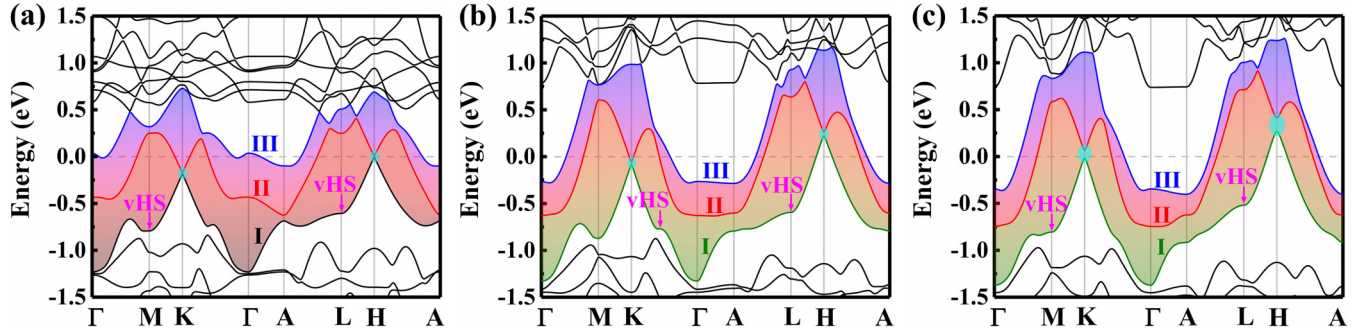


FIG. 4. Band structures with the SOC effect of (a)  $\text{CsTi}_3\text{Te}_5$ , (b)  $\text{CsZr}_3\text{Te}_5$ , and (c)  $\text{CsHf}_3\text{Te}_5$ . The colored lines indicate the bands crossing the Fermi level. The light-blue circles and the purple arrows indicate the gapped Dirac positions and the van Hove singularities, respectively. The colored shadows illustrate the continuous band gaps in the whole BZ.

Similar to the case of  $\text{CsV}_3\text{Sb}_5$  and  $\text{Au}_2\text{Pb}$  [11,84], the characters of topological nontrivial surface states and the continuous band gaps with considering the SOC effect make us easy to define the  $\text{CsZr}_3\text{Te}_5$  and  $\text{CsHf}_3\text{Te}_5$  as  $\mathbb{Z}_2$  topological metals.

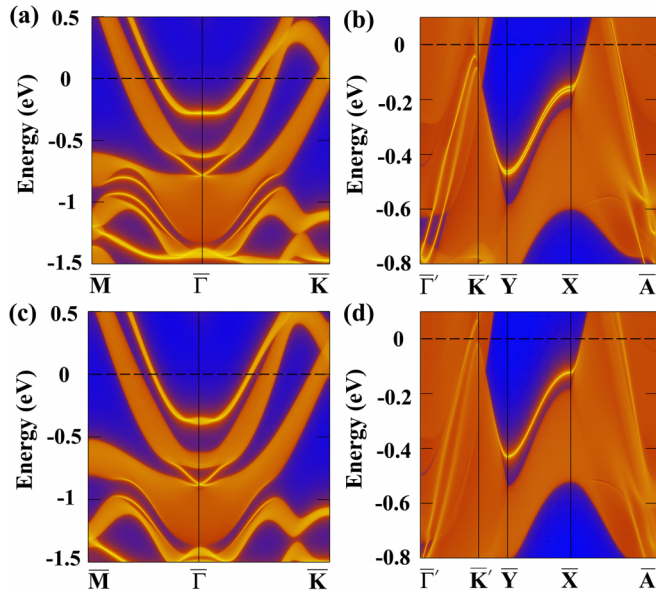


FIG. 5. Surface states in (a) (001) and (b) (100) planes for  $\text{CsZr}_3\text{Te}_5$ . (c) and (d) The same as (a) and (b) but for  $\text{CsHf}_3\text{Te}_5$ .

Materials with the coexistence of superconductivity and nontrivial band structure are promising candidates for realizing and investigating the topological superconductivity. There is an apparent disadvantage for realizing superconductivity in materials with nontrivial band structures. Normally, the DOS near the Fermi level in topological semimetals is too low to achieve a high superconducting transition temperature. In experiments, the superconductivity is induced by doping the topological insulators, such as Cu- or Nb-doped  $\text{Bi}_2\text{Se}_3$  [85,86],  $\text{Sn}_{1-x}\text{In}_x\text{Te}$  [87], etc. Compared to these doped compounds,  $\text{CsZr}_3\text{Te}_5$  and  $\text{CsHf}_3\text{Te}_5$  show intrinsic superconductivity and nontrivial topological superconductivity, which may be useful for designing novel topological superconductors.

#### IV. CONCLUSIONS

In conclusion, we systematically investigated the superconductivity and topological properties of the predicted three kagome materials  $\text{CsM}_3\text{Te}_5$ . The results of formation energy and phonon dispersion confirm their stability. According to the BCS theory, we predicted that they are medium (weak) EPC superconductors. Interestingly, the superconducting critical temperatures of these materials are obviously larger than those of the  $\text{AV}_3\text{Sb}_5$  systems. The EPC is mainly contributed by the in-plane atomic vibrations of Te and the in-plane electronic orbitals of  $M$ - $d_{xy}/d_{x^2-y^2}$  and Te  $p_x/p_y$ . Increasing the atomic number of  $M$  from Ti to Hf, the  $N(E_F)$ ,  $\lambda$ ,  $\omega_{\text{log}}$ , and

TABLE III. Parity of the wave function at TRIMs and the  $\mathbb{Z}_2$  indices of  $\text{CsM}_3\text{Te}_5$ .

Material	Band index	Parity			Product of parity			$\mathbb{Z}_2$	
		$\Gamma$	$3M$	$A$	$3L$	$\Gamma$	$3M$		$A$
$\text{CsTi}_3\text{Te}_5$	I	+	-	-	+	-	+	-	0
	II	-	+	+	-	+	+	+	0
	III	-	+	+	-	-	+	-	0
$\text{CsZr}_3\text{Te}_5$	I	+	-	+	+	-	-	-	0
	II	-	+	-	-	+	+	+	1
	III	-	-	+	-	-	+	-	0
$\text{CsHf}_3\text{Te}_5$	I	+	-	+	+	-	-	-	1
	II	-	+	-	-	+	+	+	0
	III	-	-	+	-	-	+	-	1

$T_c$  show decreasing trends. In their phonon spectra, there are many flat bands, which are responsible for the sharp peaks in the PhDOS and  $\alpha^2F(\omega)$ . At  $K$  and  $H$  points, many phonon Dirac points can be found. Without considering the SOC effect, the band structures show several Dirac-like band crossing points near the Fermi level. After including the SOC, the Dirac points are gapped, and two continuous band gaps are formed in crossing the Fermi level. The surface states on the (001) surface in the valence bands and the topological nontrivial nature clearly indicates that  $\text{CsZr}_3\text{Te}_5$  and  $\text{CsHf}_3\text{Te}_5$  are  $\mathbb{Z}_2$ -topological metals. The coexistence of superconductivity and

nontrivial band structures demonstrate that these two materials are promising platforms for exploring the relation between superconductivity and topological states in kagome materials.

#### ACKNOWLEDGMENTS

We gratefully acknowledge financial support from the National Natural Science Foundation of China (Grants No. 12104458 and No. 12074381). We also thank the computational resources from the Supercomputer Centre of the China Spallation Neutron Source.

- 
- [1] D. F. Liu, A. J. Liang, E. K. Liu, Q. N. Xu, Y. W. Li, C. Chen, D. Pei, W. J. Shi, S. K. Mo, P. Dudin, T. Kim, C. Cacho, G. Li, Y. Sun, L. X. Yang, Z. K. Liu, S. S. P. Parkin, C. Felser, and Y. L. Chen, *Science* **365**, 1282 (2019).
- [2] L. Ye, M. Kang, J. Liu, F. von Cube, C. R. Wicker, T. Suzuki, C. Jozwiak, A. Bostwick, E. Rotenberg, D. C. Bell, L. Fu, R. Comin, and J. G. Checkelsky, *Nature (London)* **555**, 638 (2018).
- [3] J. Legendre, and K. Le Hur, *Phys. Rev. Res.* **2**, 022043(R) (2020).
- [4] Y. Xing, J. Shen, H. Chen, L. Huang, Y. Gao, Q. Zheng, Y.-Y. Zhang, G. Li, B. Hu, G. Qian, L. Cao, X. Zhang, P. Fan, R. Ma, Q. Wang, Q. Yin, H. Lei, W. Ji, S. Du, H. Yang, W. Wang, C. Shen, X. Lin, E. Liu, B. Shen, Z. Wang, and H.-J. Gao, *Nat. Commun.* **11**, 5613 (2020).
- [5] T.-H. Han, J. S. Helton, S. Chu, D. G. Nocera, J. A. Rodriguez-Rivera, C. Broholm, and Y. S. Lee, *Nature (London)* **492**, 406 (2012).
- [6] S. Yan, A. Huse David, and R. White Steven, *Science* **332**, 1173 (2011).
- [7] E. Liu, Y. Sun, N. Kumar, L. Muechler, A. Sun, L. Jiao, S.-Y. Yang, D. Liu, A. Liang, Q. Xu, J. Kroder, V. Süß, H. Borrmann, C. Shekhar, Z. Wang, C. Xi, W. Wang, W. Schnelle, S. Wirth, Y. Chen, S. T. B. Goennenwein, and C. Felser, *Nat. Phys.* **14**, 1125 (2018).
- [8] Q. Wang, Y. Xu, R. Lou, Z. Liu, M. Li, Y. Huang, D. Shen, H. Weng, S. Wang, and H. Lei, *Nat. Commun.* **9**, 3681 (2018).
- [9] H. Chen, Q. Niu, and A. H. MacDonald, *Phys. Rev. Lett.* **112**, 017205 (2014).
- [10] W.-H. Ko, P. A. Lee, and X.-G. Wen, *Phys. Rev. B* **79**, 214502 (2009).
- [11] B. R. Ortiz, S. M. L. Teicher, Y. Hu, J. L. Zuo, P. M. Sarte, E. C. Schueller, A. M. M. Abeykoon, M. J. Krogstad, S. Rosenkranz, R. Osborn, R. Seshadri, L. Balents, J. He, and S. D. Wilson, *Phys. Rev. Lett.* **125**, 247002 (2020).
- [12] H. Zhao, H. Li, B. R. Ortiz, S. M. L. Teicher, T. Park, M. Ye, Z. Wang, L. Balents, S. D. Wilson, and I. Zeljkovic, *Nature (London)* **599**, 216 (2021).
- [13] C. C. Zhu, X. F. Yang, W. Xia, Q. W. Yin, L. S. Wang, C. C. Zhao, D. Z. Dai, C. P. Tu, B. Q. Song, Z. C. Tao, Z. J. Tu, C. S. Gong, H. C. Lei, Y. F. Guo, and S. Y. Li, *Phys. Rev. B* **105**, 094507 (2022).
- [14] K. Ohgushi, S. Murakami, and N. Nagaosa, *Phys. Rev. B* **62**, R6065(R) (2000).
- [15] Z. Wang, Y.-X. Jiang, J.-X. Yin, Y. Li, G.-Y. Wang, H.-L. Huang, S. Shao, J. Liu, P. Zhu, N. Shumiya, M. S. Hossain, H. Liu, Y. Shi, J. Duan, X. Li, G. Chang, P. Dai, Z. Ye, G. Xu, Y. Wang, H. Zheng, J. Jia, M. Z. Hasan, and Y. Yao, *Phys. Rev. B* **104**, 075148 (2021).
- [16] S.-L. Yu and J.-X. Li, *Phys. Rev. B* **85**, 144402 (2012).
- [17] S. Peng, Y. Han, G. Pokharel, J. Shen, Z. Li, M. Hashimoto, D. Lu, B. R. Ortiz, Y. Luo, H. Li, M. Guo, B. Wang, S. Cui, Z. Sun, Z. Qiao, S. D. Wilson, and J. He, *Phys. Rev. Lett.* **127**, 266401 (2021).
- [18] Z. Lin, C. Wang, P. Wang, S. Yi, L. Li, Q. Zhang, Y. Wang, Z. Wang, H. Huang, Y. Sun, Y. Huang, D. Shen, D. Feng, Z. Sun, J.-H. Cho, C. Zeng, and Z. Zhang, *Phys. Rev. B* **102**, 155103 (2020).
- [19] M. Li, Q. Wang, G. Wang, Z. Yuan, W. Song, R. Lou, Z. Liu, Y. Huang, Z. Liu, H. Lei, Z. Yin, and S. Wang, *Nat. Commun.* **12**, 3129 (2021).
- [20] M. Kang, L. Ye, S. Fang, J.-S. You, A. Levitan, M. Han, J. I. Facio, C. Jozwiak, A. Bostwick, E. Rotenberg, M. K. Chan, R. D. McDonald, D. Graf, K. Kaznatcheev, E. Vescovo, D. C. Bell, E. Kaxiras, J. van den Brink, M. Richter, M. Prasad Ghimire, J. G. Checkelsky, and R. Comin, *Nature Mater.* **19**, 163 (2020).
- [21] J.-X. Yin, W. Ma, T. A. Cochran, X. Xu, S. S. Zhang, H.-J. Tien, N. Shumiya, G. Cheng, K. Jiang, B. Lian, Z. Song, G. Chang, I. Belopolski, D. Multer, M. Litskevich, Z.-J. Cheng, X. P. Yang, B. Swidler, H. Zhou, H. Lin, T. Neupert, Z. Wang, N. Yao, T.-R. Chang, S. Jia, and M. Zahid Hasan, *Nature (London)* **583**, 533 (2020).
- [22] Z. Li, J. Zhuang, L. Wang, H. Feng, Q. Gao, X. Xu, W. Hao, X. Wang, C. Zhang, K. Wu, X. Dou Shi, L. Chen, Z. Hu, and Y. Du, *Sci. Adv.* **4**, eaau4511 (2018).
- [23] B. R. Ortiz, L. C. Gomes, J. R. Morey, M. Winiarski, M. Bordelon, J. S. Mangum, I. W. H. Oswald, J. A. Rodriguez-Rivera, J. R. Neilson, S. D. Wilson, E. Ertekin, T. M. McQueen, and E. S. Toberer, *Phys. Rev. Mater.* **3**, 094407 (2019).
- [24] Y. Fu, N. Zhao, Z. Chen, Q. Yin, Z. Tu, C. Gong, C. Xi, X. Zhu, Y. Sun, K. Liu, and H. Lei, *Phys. Rev. Lett.* **127**, 207002 (2021).
- [25] B. R. Ortiz, P. M. Sarte, E. M. Kenney, M. J. Graf, S. M. L. Teicher, R. Seshadri, and S. D. Wilson, *Phys. Rev. Mater.* **5**, 034801 (2021).
- [26] Y.-X. Jiang, J.-X. Yin, M. M. Denner, N. Shumiya, B. R. Ortiz, G. Xu, Z. Guguchia, J. He, M. S. Hossain, X. Liu, J. Ruff, L. Kautzsch, S. S. Zhang, G. Chang, I. Belopolski, Q. Zhang, T. A. Cochran, D. Multer, M. Litskevich, Z.-J. Cheng, X. P. Yang, Z.

- Wang, R. Thomale, T. Neupert, S. D. Wilson, and M. Z. Hasan, *Nature Mater.* **20**, 1353 (2021).
- [27] Q. Yin, Z. Tu, C. Gong, Y. Fu, S. Yan, and H. Lei, *Chin. Phys. Lett.* **38**, 037403 (2021).
- [28] F. H. Yu, T. Wu, Z. Y. Wang, B. Lei, W. Z. Zhuo, J. J. Ying, and X. H. Chen, *Phys. Rev. B* **104**, L041103 (2021).
- [29] Z. Liang, X. Hou, F. Zhang, W. Ma, P. Wu, Z. Zhang, F. Yu, J. J. Ying, K. Jiang, L. Shan, Z. Wang, and X. H. Chen, *Phys. Rev. X* **11**, 031026 (2021).
- [30] Q. Wang, P. Kong, W. Shi, C. Pei, C. Wen, L. Gao, Y. Zhao, Q. Yin, Y. Wu, G. Li, H. Lei, J. Li, Y. Chen, S. Yan, and Y. Qi, *Adv. Mater.* **33**, 2102813 (2021).
- [31] N. Shumiya, M. S. Hossain, J.-X. Yin, Y.-X. Jiang, B. R. Ortiz, H. Liu, Y. Shi, Q. Yin, H. Lei, S. S. Zhang, G. Chang, Q. Zhang, T. A. Cochran, D. Multer, M. Litskevich, Z.-J. Cheng, X. P. Yang, Z. Guguchia, S. D. Wilson, and M. Z. Hasan, *Phys. Rev. B* **104**, 035131 (2021).
- [32] Z. Zhang, Z. Chen, Y. Zhou, Y. Yuan, S. Wang, J. Wang, H. Yang, C. An, L. Zhang, X. Zhu, Y. Zhou, X. Chen, J. Zhou, and Z. Yang, *Phys. Rev. B* **103**, 224513 (2021).
- [33] F. H. Yu, D. H. Ma, W. Z. Zhuo, S. Q. Liu, X. K. Wen, B. Lei, J. J. Ying, and X. H. Chen, *Nat. Commun.* **12**, 3645 (2021).
- [34] K. Y. Chen, N. N. Wang, Q. W. Yin, Y. H. Gu, K. Jiang, Z. J. Tu, C. S. Gong, Y. Uwatoko, J. P. Sun, H. C. Lei, J. P. Hu, and J. G. Cheng, *Phys. Rev. Lett.* **126**, 247001 (2021).
- [35] L. Yin, D. Zhang, C. Chen, G. Ye, F. Yu, B. R. Ortiz, S. Luo, W. Duan, H. Su, J. Ying, S. D. Wilson, X. Chen, H. Yuan, Y. Song, and X. Lu, *Phys. Rev. B* **104**, 174507 (2021).
- [36] Y. Song, T. Ying, X. Chen, X. Han, X. Wu, A. P. Schnyder, Y. Huang, J.-g. Guo, and X. Chen, *Phys. Rev. Lett.* **127**, 237001 (2021).
- [37] T. Wang, A. Yu, H. Zhang, Y. Liu, W. Li, W. Peng, Z. Di, D. Jiang, and G. Mu, [arXiv:2105.07732](https://arxiv.org/abs/2105.07732).
- [38] B. Q. Song, X. M. Kong, W. Xia, Q. W. Yin, C. P. Tu, C. C. Zhao, D. Z. Dai, K. Meng, Z. C. Tao, Z. J. Tu, C. S. Gong, H. C. Lei, Y. F. Guo, X. F. Yang, and S. Y. Li, [arXiv:2105.09248](https://arxiv.org/abs/2105.09248).
- [39] B. R. Ortiz, S. M. L. Teicher, L. Kautzsch, P. M. Sarte, N. Ratcliff, J. Harter, J. P. C. Ruff, R. Seshadri, and S. D. Wilson, *Phys. Rev. X* **11**, 041030 (2021).
- [40] S. Kobayashi and M. Sato, *Phys. Rev. Lett.* **115**, 187001 (2015).
- [41] X.-H. Tu, P.-F. Liu, W. Yin, J.-R. Zhang, P. Zhang, and B.-T. Wang, *Mater. Today Phys.* **24**, 100674 (2022).
- [42] X.-L. Qi and S.-C. Zhang, *Rev. Mod. Phys.* **83**, 1057 (2011).
- [43] A. Y. Kitaev, *Ann. Phys. (NY)* **303**, 2 (2003).
- [44] P. Ding, C. H. Lee, X. Wu, and R. Thomale, *Phys. Rev. B* **105**, 174518 (2022).
- [45] W. L. McMillan, *Phys. Rev.* **167**, 331 (1968).
- [46] P. B. Allen and R. C. Dynes, *Phys. Rev. B* **12**, 905 (1975).
- [47] P. Giannozzi, S. Baroni, N. Bonini, M. Calandra, R. Car, C. Cavazzoni, D. Ceresoli, G. L. Chiarotti, M. Cococcioni, I. Dabo, A. Dal Corso, S. de Gironcoli, S. Fabris, G. Fratesi, R. Gebauer, U. Gerstmann, C. Gougoussis, A. Kokalj, M. Lazzeri, L. Martin-Samos, N. Marzari, F. Mauri, R. Mazzarello, S. Paolini, A. Pasquarello, L. Paulatto, C. Sbraccia, S. Scandolo, G. Sclauzero, A. P. Seitsonen, A. Smogunov, P. Umari, and R. M. Wentzcovitch, *J. Phys.: Condens. Matter* **21**, 395502 (2009).
- [48] D. Vanderbilt, *Phys. Rev. B* **41**, 7892 (1990).
- [49] J. P. Perdew, K. Burke, and M. Ernzerhof, *Phys. Rev. Lett.* **77**, 3865 (1996).
- [50] S. Grimme, J. Antony, S. Ehrlich, and H. Krieg, *J. Chem. Phys.* **132**, 154104 (2010).
- [51] H. Tan, Y. Liu, Z. Wang, and B. Yan, *Phys. Rev. Lett.* **127**, 046401 (2021).
- [52] J.-G. Si, W.-J. Lu, Y.-P. Sun, P.-F. Liu, and B.-T. Wang, *Phys. Rev. B* **105**, 024517 (2022).
- [53] Z. Liu, N. Zhao, Q. Yin, C. Gong, Z. Tu, M. Li, W. Song, Z. Liu, D. Shen, Y. Huang, K. Liu, H. Lei, and S. Wang, *Phys. Rev. X* **11**, 041010 (2021).
- [54] S. Baroni, S. de Gironcoli, A. Dal Corso, and P. Giannozzi, *Rev. Mod. Phys.* **73**, 515 (2001).
- [55] L. Yan, B.-T. Wang, X. Huang, Q. Li, K. Xue, J. Zhang, W. Ren, and L. Zhou, *Nanoscale* **13**, 18947 (2021).
- [56] M. J. Verstraete, M. Torrent, F. Jollet, G. Zérah, and X. Gonze, *Phys. Rev. B* **78**, 045119 (2008).
- [57] M. P. L. Sancho, J. M. L. Sancho, J. M. L. Sancho, and J. Rubio, *J. Phys. F: Met. Phys.* **15**, 851 (1985).
- [58] Q. Wu, S. Zhang, H.-F. Song, M. Troyer, and A. A. Soluyanov, *Comput. Phys. Commun.* **224**, 405 (2018).
- [59] I. Souza, N. Marzari, and D. Vanderbilt, *Phys. Rev. B* **65**, 035109 (2001).
- [60] N. Marzari, A. A. Mostofi, J. R. Yates, I. Souza, and D. Vanderbilt, *Rev. Mod. Phys.* **84**, 1419 (2012).
- [61] H. Lin, G. Tan, G.-N. Shen, S. Hao, L.-M. Wu, M. Calta, C. Malliakas, S. Wang, C. Uher, C. Wolverton, and M. G. Kanatzidis, *Angew. Chem.* **128**, 11603 (2016).
- [62] N. Ma, F. Jia, L. Xiong, L. Chen, Y. Y. Li, and L. M. Wu, *Inorg. Chem.* **58**, 1371 (2019).
- [63] N. Ma, Y. Y. Li, L. Chen, and L. M. Wu, *J. Am. Chem. Soc.* **142**, 5293 (2020).
- [64] Y. Jiang, Z. Yu, Y. Wang, T. Lu, S. Meng, K. Jiang, and M. Liu, *Chin. Phys. Lett.* **39**, 047402 (2022).
- [65] See Supplemental Material at <http://link.aps.org/supplemental/10.1103/PhysRevB.106.214527> for the methods and results of structure search.
- [66] Y.-C. Wang, J. Lv, L. Zhu, and Y.-M. Ma, *Phys. Rev. B* **82**, 094116 (2010).
- [67] Y.-C. Wang, J. Lv, L. Zhu, and Y.-M. Ma, *Comput. Phys. Commun.* **183**, 2063 (2012).
- [68] D. J. Wales, *Chem. Phys. Lett.* **285**, 330 (1998).
- [69] S. Baroni, P. Giannozzi, and A. Testa, *Phys. Rev. Lett.* **58**, 1861 (1987).
- [70] P. Giannozzi, S. de Gironcoli, P. Pavone, and S. Baroni, *Phys. Rev. B* **43**, 7231 (1991).
- [71] G. Kresse and J. Furthmüller, *Phys. Rev. B* **54**, 11169 (1996).
- [72] A. Togo and I. Tanaka, *Scr. Mater.* **108**, 1 (2015).
- [73] C. Adenis, V. Langer, and O. Lindqvist, *Acta Crystallogr. Sec. C* **45**, 941 (1989).
- [74] H. Ryu, Y. Chen, H. Kim, H.-Z. Tsai, S. Tang, J. Jiang, F. Liou, S. Kahn, C. Jia, A. A. Omrani, J. H. Shim, Z. Hussain, Z.-X. Shen, K. Kim, B. I. Min, C. Hwang, M. F. Crommie, and S.-K. Mo, *Nano Lett.* **18**, 689 (2018).
- [75] J. G. Si, M. J. Wei, H. Y. Wu, R. C. Xiao, and W. J. Lu, *Europhys. Lett.* **127**, 37001 (2019).
- [76] B.-T. Wang, P.-F. Liu, J.-J. Zheng, W. Yin, and F. Wang, *Phys. Rev. B* **98**, 014514 (2018).
- [77] J. Kortus, I. I. Mazin, K. D. Belashchenko, V. P. Antropov, and L. L. Boyer, *Phys. Rev. Lett.* **86**, 4656 (2001).

- [78] X.-W. Yi, X.-Y. Ma, Z. Zhang, Z.-W. Liao, J.-Y. You, and G. Su, [arXiv:2202.05588](https://arxiv.org/abs/2202.05588).
- [79] J. Bardeen, L. N. Cooper, and J. R. Schrieffer, *Phys. Rev.* **108**, 1175 (1957).
- [80] J. Bardeen, L. N. Cooper, and J. R. Schrieffer, *Phys. Rev.* **106**, 162 (1957).
- [81] B.-T. Wang, P. Zhang, H.-Y. Liu, W.-D. Li, and P. Zhang, *J. Appl. Phys.* **109**, 063514 (2011).
- [82] T. Bo, P.-F. Liu, L. Yan, and B.-T. Wang, *Phys. Rev. Mater.* **4**, 114802 (2020).
- [83] T. Machida, Y. Sun, S. Pyon, S. Takeda, Y. Kohsaka, T. Hanaguri, T. Sasagawa, and T. Tamegai, *Nature Mater.* **18**, 811 (2019).
- [84] L. M. Schoop, L. S. Xie, R. Chen, Q. D. Gibson, S. H. Lapidus, I. Kimchi, M. Hirschberger, N. Haldolaarachchige, M. N. Ali, C. A. Belvin, T. Liang, J. B. Neaton, N. P. Ong, A. Vishwanath, and R. J. Cava, *Phys. Rev. B* **91**, 214517 (2015).
- [85] Y. S. Hor, A. J. Williams, J. G. Checkelsky, P. Roushan, J. Seo, Q. Xu, H. W. Zandbergen, A. Yazdani, N. P. Ong, and R. J. Cava, *Phys. Rev. Lett.* **104**, 057001 (2010).
- [86] T. Asaba, B. J. Lawson, C. Tinsman, L. Chen, P. Corbae, G. Li, Y. Qiu, Y. S. Hor, L. Fu, and L. Li, *Phys. Rev. X* **7**, 011009 (2017).
- [87] G. Balakrishnan, L. Bawden, S. Cavendish, and M. R. Lees, *Phys. Rev. B* **87**, 140507(R) (2013).